Benjamin Pannetier, Jean Dezert
The French Aerospace Lab.,
ONERA/DTIM/SIF,
29 Avenue de la Division Leclerc,
92320 Châtillon, France.
benjamin.pannetier@onera.fr, jean.dezert@onera.fr

Improvement of multiple ground targets tracking with fusion of identification attributes

Published in:
Florentin Smarandache & Jean Dezert (Editors)
Advances and Applications of DSmT for Information Fusion
(Collected works), Vol. III
American Research Press (ARP), Rehoboth, 2009
ISBN-10: 1-59973-073-1
ISBN-13: 978-1-59973-073-8
Chapter XIV, pp. 661 - 690

Abstract: *Multiple ground targets (MGT) tracking is a challenging problem in real environment. Advanced algorithms include exogeneous information like road network and terrain topography. In this chapter, we develop a new improved VS-IMM (Variable Structure Interacting Multiple Model) algorithm for GMTI (Ground Moving Target Indicator) and IMINT (IMagery INTelligence) tracking which includes the stop-move target maneuvering model, contextual information (on-off road model, road network constraints), and ID (IDentification) information arising from classifiers coupled with the GMTI sensor. The identification information is integrated to the likelihood of each hypothesis of our SB-MHT (Structured Branching - Multiple Hypotheses Tracking). We maintain aside each target track a set of ID hypotheses with their committed beliefs which are updated on real time with classifier decisions through target type tracker based on a proportional conflict redistribution fusion rule developed in DSmT. The advantage of such a new approach is to deal precisely and efficiently with the identification attribute information available as it comes by taking into account its inherent uncertainty/non-specificity and possible high auto-conflict.*

24.1 Introduction

Data fusion for ground battlefield surveillance is more and more strategic in order to create the situational assessment or improve the precision of fire control system. The challenge of data fusion for the theatre surveillance operation is to know where are the targets, how they evolve (maneuvers, group formations,...) and what are their identities. For the first two questions, we develop new ground target tracking algorithms adapted to GMTI (Ground Moving Target Indicator) sensors. In fact, GMTI sensors are able to cover a large surveillance area during few hours or more if several sensors exist. However, ground target tracking algorithms are used in a complex environment due to the high traffic density and the false alarms that generate a significant data quantity, the terrain topography which can provocate non-detection areas for the sensor and the high maneuverability of the ground targets which yields to the data association problem. Several references exist for the MGT (Multiple Ground Targets) tracking with GMTI sensors [6, 9] which fuse contextual informations with MTI reports. The main results are the improvement of the track precision and track continuity. Our algorithm [13] is built with several reflexions inspired with this literature. Based on road segment positions, dynamic motion models under road constraint are built and an optimized projection of the estimated target states is proposed to keep the track on the road. A VS-IMM (Variable Structure Interacting Multiple Models) filter is created with a set of constrained models to deal with the target maneuvers on the road. The set of models used in the variable structure is adjusted sequentially according to target positions and to the road network topology.

Now, we extended the MGT with several sensors. In this chapter, we first consider the centralized fusion between GMTI and IMINT (IMagery INTelligence) sensors reports. The first problem of the data fusion with several sensors is the data registration in order to work in the same geographic and time referentials. This point is not presented in this chapter. However, in a multisensor system, measurements can arrive out of sequence. Following Bar-Shalom and Chen's works [3], the VS-IMMC (VS-IMM Constrained) algorithm is adapted to the OOSM (Out Of Sequence Measurement) problem, in order to avoid the reprocessing of entire sequence of measurements. The VS-IMMC is also extended in a multiple target context and integrated in a SB-MHT (Structured Branching - Multiple Hypotheses Tracking). Despite of the resulting track continuity improvement for the VS-IMMC SB-MHT algorithm, unavoidable association ambiguities arise in a multi-target context when several targets move in close formation (crossing and passing). The associations between all constrained predicted states are compromised if we use only the observed locations as measurements. The weakness of this algorithm is due to the lack of good target state discrimination.

One way to enhance data associations is to use the reports classification attribute. In our previous work [14], the classification information of the MTI segments has been introduced in the target tracking process. The idea was to maintain aside each target track a set of ID hypotheses. Their committed beliefs are revised in real time with the

classifier decision through a very recent and efficient fusion rule called proportional conflict redistribution (PCR). In this chapter, in addition to the measurement location fusion, a study is carried out to fuse MTI classification type with image classification type associated to each report. The attribute type of the image sensors belongs to a different and better classification than the MTI sensors. The counterpart is the short coverage of image sensors that brings about a low data quantity. In section 24.2, the motion and measurement models are presented with a new ontologic model in order to place the different classification frames in the same frame of discernment. After the VS-IMMC description given in section 24.4, the PCR fusion rule originally developed in DSmT (Dezert-Smarandache Theory) framework is presented in section 24.5 to fuse the target type information available and to include the resulting fused target ID into the tracking process. The last part of this chapter is devoted to simulation results for a multiple target tracking scenario within a real environment.

24.2 Motion model

24.2.1 Introduction

Usual target tracking algorithms are based on the Kalman filter. Since several years, in ground target tracking domain, the Kalman filter has been improved to take into account the contextual information in the tracking process. For instance, Kirubarajan *et al.* proposed to use the road segment location in order to modelize the dynamic of a target moving on the road [9]. The road network is considered here as *a priori* information to be integrated in the tracking system. The map information comes from a GIS (Geographic Information System) which contains information about the road network location and the DTED (Digital Terrain Elevation Data). In the following, the GIS description, the stochastic target constrained and the measurement models are presented.

24.2.2 GIS description

The GIS used in this work contains the following information: the segmented road network and DTED. Each road segment is expressed in the WGS84 system. The road network is connected and each road segment is indexed by the road section it belongs to. A road section $Ro(p)$ is defined by a connected road segments set delimited by a road end or a junction in the manner that $Ro(p) = \{s_0, s_1, \cdots\}$.

At the beginning of a surveillance battlefield operation, a Topographic Coordinate Frame (TCF) and its origin O are chosen in the manner that the axes X, Y and Z are respectively oriented in the East, North and Up local directions. The target tracking process is carried out in the TCF.

24.2.3 Target state under constraint

24.2.3.1 Constrained motion model

The target state at the current time k is defined in the local coordinate frame by[1]:

$$\mathbf{x}(k) = [x(k)\, \dot{x}(k)\, y(k)\, \dot{y}(k)]' \tag{24.1}$$

where the couples $(x(k), y(k))$ and $(\dot{x}(k), \dot{y}(k))$ define respectively the target location and velocity. The dynamics of the targets evolving on the road network are modelized by a first-order system.

The target state under the road segment s is defined by

$$\mathbf{x}_s(k) = [x_s(k)\, \dot{x}_s(k)\, y_s(k)\, \dot{y}_s(k)]' \tag{24.2}$$

where the target position $(x_s(k), y_s(k))$ belongs to the road segment and the corresponding velocity vector $(\dot{x}_s(k), \dot{y}_s(k))$ is in the road segment s direction. Therefore, the target constraint state $\mathbf{x}_s(k)$ is defined by the following constraint:

$$\begin{cases} a \cdot x_s(k) + b \cdot y_s(k) + c = 0 \\ \langle [\dot{x}(k)\, \dot{y}(k)]' \, | \vec{n}_s \rangle = 0 \end{cases} \tag{24.3}$$

where a, b and c are the coefficients of the line associated to the road segment s and $\vec{n}_s$ is the normal vector to the road segment s. The constraint can be expressed as follows:

$$\tilde{\mathbf{D}} \cdot \mathbf{x}_s(k) = \mathbf{L} \tag{24.4}$$

with $\tilde{\mathbf{D}} = \begin{bmatrix} a & 0 & b & 0 \\ 0 & a & 0 & b \end{bmatrix}$ and $\mathbf{L} = [-c\ 0]'$.

The event that the target is on the road segment s is noted $e_s(k) = \{(x(k), y(k)) \in s\}$. Knowing the event $e_s(k)$ and according to a motion model M_i the dynamics of the target can be improved by considering the road segment s. Due to the precision of the GMTI sensor and the long time scan period, the chosen motion models are quite simple. They consist in r constant velocity motion models having different process noise statistics (standard deviations). However the proposed approach is valid for much more complicated motion models like the constant acceleration or coordinated turn ones. It follows that:

$$\mathbf{x}_s(k) = \mathbf{F}_{s,i}(\Delta_k) \cdot \mathbf{x}_s(k-1) + \mathbf{\Gamma}(\Delta_k) \cdot \boldsymbol{\nu}_{s,i}(k) \tag{24.5}$$

where Δ_k is the time of sampling; the matrix $\mathbf{F}_{s,i}(k) \triangleq \mathbf{F}_{s,i}(\Delta_k)$ is the state transition matrix associated to the road segment s (described in [12]) and is adapted to a motion model M_i; The matrix $\mathbf{\Gamma}(\Delta_k)$ is defined in [1] and the variable $\boldsymbol{\nu}_{s,i}(k)$ is a white noise Gaussian process. Its associated covariance $\mathbf{Q}_{s,i}(k)$ is built in the manner that the

[1] $\mathbf{x}'$ denotes the transposition of the vector (or the matrix) $\mathbf{x}$.

standard deviation σ_n along the road segment is higher than the standard deviation σ_d in the orthogonal direction. Consequently the covariance matrix $\mathbf{Q}_{s,i}$ is defined by:

$$\mathbf{Q}_{s,i}(k) = \mathbf{R}_{\vartheta_s} \cdot \begin{bmatrix} \sigma_d^2 & 0 \\ 0 & \sigma_n^2 \end{bmatrix} \cdot \mathbf{R}'_{\vartheta_s} \tag{24.6}$$

where the matrix $\mathbf{R}_{\vartheta_s}$ is the rotation matrix associate to the s road segment direction ϑ_s defined in the plane (O, X, Y). The predicted target state and covariance are defined respectively by:

$$\hat{\mathbf{x}}_{s,i}(k|k-1) = \mathbf{F}_{s,i}(k) \cdot \hat{\mathbf{x}}_{s,i}(k-1|k-1) \tag{24.7}$$

$$\mathbf{P}_{s,i}\,(k\,|k-1\,) = \mathbf{F}_{s,i}\,(k) \cdot \mathbf{P}_{s,i}(k-1|k-1) \cdot \mathbf{F}'_{s,i}(k) + \mathbf{Q}_{s,i}(k) \tag{24.8}$$

24.2.3.2 Adjustment of the process noise at the road extremities

Since the previous constraint on the motion model is specific only to a given segment s, it does not take into account the whole road network[2] and thus it omits the possibility for the target to switch onto another road segment when reaching the extremity of the segment it is moving on. Such modeling is too simplistic and the ground-target tracking based on it provides in general poor performances. To improve modeling for targets moving on a road network, we propose to adapt the level of the dynamic model's noise depending on the length of the road segment s and on the location of the target on this segment with respect to its extremities. This allows to relax gradually the on-segment constraint as soon as the target approaches the extremity of the road segment and/or a junction. If we omit the road segment length in the motion model, the tracking algorithm may not associate the predicted track with a measurement when the predicted state is near the road segment extremity. In fact, if a measurement is originated from a target moving on the road segment $s+1$, the measurement won't be in the validation gate (defined in [5]), because of the road segment s constraint that generates a directive predicted covariance with a small standard deviation in the road segment s orthogonal direction. That is why, we propose to increase the standard deviation σ_d when the target approaches the road extremity, in the manner that the standard deviation in the orthognal road segment direction becomes equal to the standard deviation in the road segment direction. For this, we use the *prior* probability $P\{e_s(k)|\mathbf{Z}^{k-1,n}\}$ in order to relax the constraint when the target approaches the road segment s extremity. The white noise Gaussian process $\nu_{s,i}(k)$ in (24.5) is modified in the manner that the covariance $\mathbf{Q}_{s,i}$ is replaced by $\tilde{\mathbf{Q}}_{s,i}$:

$$\tilde{\mathbf{Q}}_{s,i}(k) = \mathbf{R}_{\vartheta_s} \cdot \begin{bmatrix} \sigma_d^2 & 0 \\ 0 & q_{22} \end{bmatrix} \cdot \mathbf{R}'_{\vartheta_s} \tag{24.9}$$

[2] *i.e.* the possibility of several other road segments connected at extremity of each road segment of the network.

where $q_{22} = \sigma_n^2 \cdot P\{e_s(k)|\mathbf{Z}^{k-1}\} + \sigma_d^2 \cdot (1 - P\{e_s(k)|\mathbf{Z}^{k-1}\}$ and $\mathbf{Z}^{k-1}$ is the sequence of measurements up to time $k-1$.

The probability that the target belongs to the road segment s is based on the derivations proposed by Ulmke and Koch [19] and Herrero *et al.* [8], but we do not consider the road width and our modelization is done in the 2D space only. So the predicted road segment s belonging probability is expressed as:

$$P\{e_s(k)|\mathbf{Z}^{k-1,n}\} = \begin{cases} 0, \text{if } \Pi_s(\mathbf{x}(k)) \leq 0 \text{ or } \Pi_s(\mathbf{x}(k)) \geq l_s, \\ P\{\Pi_s(\mathbf{x}(k)) \leq l_s \mid \mathbf{Z}^{k-1,n}\}, \text{otherwise.} \end{cases} \tag{24.10}$$

where $\Pi_s(x(k))$ is the projection operator on the road segment s modulo the road segment length l_s. According to the Gaussian assumption, the probability can be rewritten as follows:

$$\begin{aligned} P\{e_s(k)|\mathbf{Z}^{k-1,n}\} &= \int_0^{l_s} \mathcal{N}\left(u, \Pi_s\left(\mathbf{x}(k)\right), \sigma_s^2\right) du \\ &= f\left(\frac{l_s - \prod_s(\mathbf{x}(k))}{\sigma_s}\right) - f\left(\frac{-\prod_s(\mathbf{x}(k))}{\sigma_s}\right) \end{aligned} \tag{24.11}$$

The variance σ_s^2 is the variance obtained after the projection Π_s on the road segment s and is given in [19]. The function $f(.)$ is the integral of the Gaussian distribution with zero mean and variance of $1/2$:

$$f(t) = \frac{1}{\sqrt{2\pi}} \cdot \int_{-\infty}^{t} e^{-\frac{t^2}{2}} dt \tag{24.12}$$

Finally, we obtain a constrained motion model which takes into account the uncertainty that the target belongs to the road segment. This uncertainty is modelized by an additive noise process.

24.2.3.3 Constrained state estimation

We define $M_s^i(k) = \left\{M^i(k) \cap e_s(k)\right\}$ the event that the target is following a dynamic according to the motion model M^i and moves on the road segment s. So, the state probability density function (*i.e.* pdf) given the measurements set $\mathbf{Z}^k$ and the event $M_s^i(k)$ is denoted :

$$p(\mathbf{x}(k)|\mathbf{Z}^k, \theta^{k,l}, M_s^i(k)) \tag{24.13}$$

The state $\mathbf{x}_i(k)$ is a Gaussian random vector defined by its estimated mean $\hat{\mathbf{x}}_i(k|k)$ and its estimated covariance $\mathbf{P}_i(k|k)$ (both obtained using a model based filter). Under the road constraint, the estimated state $\hat{\mathbf{x}}_{s,i}(k|k)$ is therefore obtained by the maximization of pdf (24.3) given the event M_s^i. Finally, under the Gaussian assumption of the Kalman filter, the analytic expression of the constrained estimate state associate with the motion model M^i is obtained by calculating the Lagrangian

of (24.3) under the constraint (24.4). The expressions of the constrained estimated state and its covariance are given in [13]:

$$\hat{\mathbf{x}}_{i,s}(k|k) = \hat{\mathbf{x}}_i(k|k) - \mathbf{P}_{\mathrm{i}}(k|k) \cdot \tilde{\mathbf{D}} \cdot (\tilde{\mathbf{D}}\mathbf{P}_i(k|k)\tilde{\mathbf{D}}')^{-1} \cdot (\tilde{\mathbf{D}}\hat{\mathbf{x}}_i(k|k) - \mathbf{L}) \tag{24.14}$$

$$\mathbf{P}_{i,s}(k|k) = (\mathbf{Id} - \mathbf{W}(k)) \cdot \mathbf{P}_i(k|k) \cdot (\mathbf{Id} - \mathbf{W}(k))' \tag{24.15}$$

where the matrix **Id** is the identity matrix and $\mathbf{W}(k)$ is defined by:

$$\mathbf{W}(k) = \mathbf{P}_i(k|k) \cdot \tilde{\mathbf{D}}' \cdot (\tilde{\mathbf{D}} \cdot \mathbf{P}_i(k|k) \cdot \tilde{\mathbf{D}}') \cdot \tilde{\mathbf{D}} \tag{24.16}$$

Since the road network is composed of several road segments and a ground target has several motion models, we consider an IMM (Interacting Multiple Model) with a variable structure [1] to adapt the constraint motion models set to the road network configuration. This VS-IMMC is presented in the section 24.4.

24.3 Measurement model

24.3.1 GMTI model

24.3.1.1 MTI report model

According to the NATO GMTI formats, the MTI reports are expressed in WGS84 coordinates system [11]. All MTI reports are converted for each tracking station into the TCF. A (noise-free) MTI measurement vector $\mathbf{z}_{mti}(k)$ at the current time k is given in the TCF by:

$$\mathbf{z}_{mti}(k) = [x(k)\, y(k)\, \dot{\rho}(k)]' \tag{24.17}$$

where $(x(k), y(k))$ are the x and y MTI coordinates in the local frame $(0, X, Y)$ and $\dot{\rho}_m$ is the associated range-rate expressed in the TCF as:

$$\dot{\rho}(k) = \frac{(x(k) - x_c(k)) \cdot \dot{x}(k) + (y(k) - y_c(k)) \cdot \dot{y}(k)}{\sqrt{(x(k) - x_c(k))^2 + (y(k) - y_c(k))^2}} \tag{24.18}$$

where $(x_c(k), y_c(k))$ is the sensor location at the current time in the TCF. The range radial velocity is correlated to the MTI location components, so the use of an extended Kalman filter (EKF) is not adapted. In literature, there exist several techniques to uncorrelate the range-rate from the location components like for example, the SEKF from Wang *et al.* [21] based on Cholesky's decomposition. Nevertheless, we prefer to use the AEKF (Alternative Extended Kalman Filter) presented by Bizup and Brown [4]. This last one is very simple to compute because the authors propose only to use an alternative linearization of the EKF (Extended Kalman Filter). Moreover, AEKF working in the sensor referential/frame remains invariant by translation. Then, the measurement equation is given according to the AEKF, by:

$$\mathbf{z}_{mti}(k) = \mathbf{H}_{mti}(k) \cdot \mathbf{x}(k) + \boldsymbol{\nu}_{mti}(k) \tag{24.19}$$

where $\boldsymbol{\nu}_{mti}(k)$ is a zero-mean white Gaussian noise vector and $\mathbf{H}(k)$ is given by:

$$\mathbf{H}_{mti}(k) = \begin{bmatrix} 1 & 0 & 0 & 0 \\ 0 & 0 & 1 & 0 \\ 0 & \frac{\partial \dot{\rho}(k)}{\partial \dot{x}} & 0 & \frac{\partial \dot{\rho}(k)}{\partial \dot{y}} \end{bmatrix} \tag{24.20}$$

The explicit expression of (24.20) is given in [4].

24.3.1.2 MTI Classification segment

An issue to improve the multiple target tracking algorithm is to combine the kinematic data association with the attribute data association. In the STANAG 4607 [11], each MTI report is associated to the location and velocity information (described in the previous part) in addition to the attribute information with its probability that it is correct. We denote $C_{MTI} = \{c_0, c_1, \ldots, c_u\}$, the frame of discernement of our target classification problem. C_{MTI} is assumed to be constant over time (*i.e.* target ID does not change with time) and consists of a finite set of u exhaustive and exclusive elements representing the possible states of the world for target classification. In the STANAG 4607 the set C_{MTI} is defined by :

$$C_{MTI} = \left\{ \begin{array}{l} No\ Information, \\ Tracked\ Vehicle, \\ Wheeled\ Vehicle, \\ Rotary\ Wing\ Aircraft, \\ Fixed\ Wing\ Aircraft, \\ StationaryRotator, \\ Maritime, \\ Beacon, \\ Amphibious \end{array} \right\} \tag{24.21}$$

In addition to the classification or attribute information, the STANAG allows to use the probability $P\{c(k)\}$, $(\forall c(k) \in C_{MTI})$, but it does not specify the way these probabilities are obtained because $P\{c(k)\}$ are actually totally dependent on the algorithm chosen for target classification. In this chapter, we do not focus on the classification algorithm itself, but rather on how to improve multiple ground targets tracking with attribute information and target classification. Hence, we consider the probabilities $P\{c(k)\}$ as input parameters of our tracking system characterizing the global performances of the classifier. In other words, $P\{c(k)\}$, $(\forall c(k) \in C_{MTI})$, represent the diagonal terms of the confusion matrix C_{MTI} of the classification algorithm assumed to be used. The modified/extended measurement $\mathbf{z}^{\star}_{mti}(k)$ including both kinematic part and (classification) attribute part is defined as:

$$\mathbf{z}^{\star}_{mti}(k) = \{z_{mti}(k), c(k), P\{c(k)\}\} \tag{24.22}$$

24.3.2 IMINT model

For the imagery intelligence (IMINT), we consider two sensor types : a video EO/IR sensor carried by a Unmanned Aerial Vehicle (UAV) and a EO sensor fixed on a Unattended Ground Sensor (UGS).

24.3.2.1 EO/IR report model

We assume that the video information given by both sensor types are processed by their own ground stations and that the system provides the video reports of target detections with their classification attributes. Moreover, a human operator selects targets on a movie frame and is able to choose its attribute with a HMI (Human Machine Interface). In addition, the operator is able with the UAV to select *several targets* on a frame. On the contrary, the operator selects *only one target* with the frames given by the UGS. There is *no false alarm* and a target cannot be detected by the operator (due to terrain mask for example). The video report on the movie frame is converted in the TCF. The measurement equation is given by:

$$\mathbf{z}_{video}(k) = \mathbf{H}_{video}(k) \cdot \mathbf{x}(k) + \mathbf{w}_{video}(k) \tag{24.23}$$

where $\mathbf{H}_{video}$ is the observation matrix of the video sensor

$$\mathbf{H}_{video} = \begin{bmatrix} 1 & 0 & 0 & 0 \\ 0 & 0 & 1 & 0 \end{bmatrix} \tag{24.24}$$

The white noise Gaussian process $\mathbf{w}_{video}(k)$ is centered and has a known covariance $\mathbf{R}_{video}(k)$ given by the ground station.

24.3.2.2 EO/IR classification segment

Each video report is associated to the attribute information $c(k)$ with its probability $P\{c(k)\}$ that it is correct. We denote C_{video} the frame of discernment for an EO/IR source. As C_{MTI}, C_{video} is assumed to be constant over the time and consists of a finite set of exhaustive and exclusive elements representing the possible states of the target classification. In this chapter, we consider only eight elements in C_{video} as follows:

$$C_{video} = \left\{ \begin{array}{l} Civilian\ Car, \\ Military\ Armoured\ Car, \\ Wheeled\ Armoured\ Vehicle, \\ Civilian\ Bus, \\ Military\ Bus, \\ Civilian\ Truck, \\ Military\ Armoured\ Truck, \\ Helicopter \end{array} \right\} \tag{24.25}$$

Let $\mathbf{z}^{\star}_{video}(k)$ be the extended video measurements including both kinematic part and attribute part expressed by the following formula among $m(k)$ measurements

$(\forall c(k) \in C_{video})$:

$$\mathbf{z}^{\star}_{video}(k) \triangleq \{\mathbf{z}_{video}(k), c(k), P\{c(k)\}\} \tag{24.26}$$

24.3.3 Ontologic model

In our work, the symbology APP-6A [18] is used to describe the links between the different classification sets (24.21) and (24.25). The figure 24.1 represents a short part of the APP-6 A used in this chapter. Each element of both sets can be placed in 24.1. For example, the wheeled vehicle of the set C_{MTI} is placed at the level 1.X.3.1.1.2.2 and the military armoured truck of the set $_{video}$ is placed at the level 1.X.3.1.1.2.1. Finally, all attribute elements are committed to a level in the APP-6A.

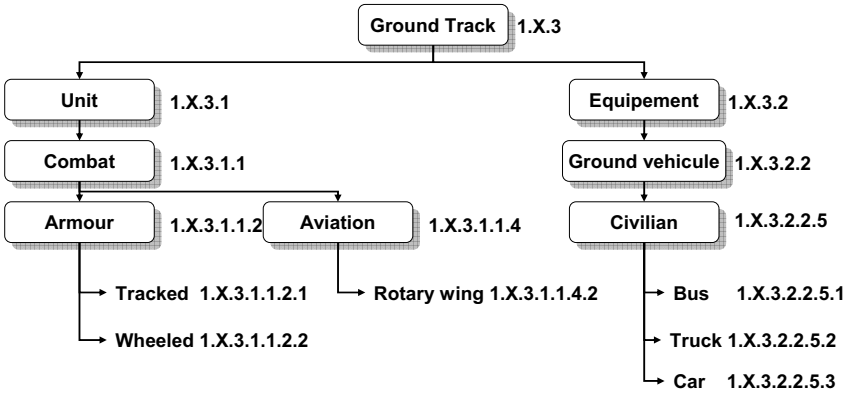

Figure 24.1: APP-6A (light version).

24.4 VS-IMM with road constraints (VS-IMMC)

24.4.1 Track definitions and notations

Let's denote $\mathcal{T}(k)$ the set of all tracks present at the current time. In the following of the article, the event $\theta^{k,l}$ is associated to the l^{th} sequential measurements $\mathbf{Z}^{k,l}$ and represents the set of measurements generated by the target. In addition, it exists a subsequence n and a measurement j $(\forall j \in \{1, \ldots, m_k\})$ in the manner that $\mathbf{Z}^{k,l} = \{\mathbf{Z}^{k-1,n}, ..., \mathbf{z}_j(k)\}$ is the measurements sequence associates to the track $\mathbf{T}^{k,l}$. We recall that a track is an estimated states sequence expressed by the following expression: $\forall l \in \{1, \cdots, |\mathcal{T}(k)|\}, \exists! s \in \{1, \cdots, |\mathcal{T}(k-1)|\}$, such that

$$\mathbf{T}^{k,l} = \{(\hat{\mathbf{x}}^{l}(k|k), \mathbf{P}^{l}(k|k)), \mathbf{T}^{k-1,s}\} \tag{24.27}$$

A track family $\tau_n(k)$ at the current time k represents a data collection of tracks $\mathbf{T}^{k,l}$ $(\exists l \in \{1, \cdots, |\mathcal{T}(k)|\})$ generated by the same measurement $\mathbf{z}_j(k_0)$ at time t_{k_0}. A track family must be associated to only one target and represents the differents association hypotheses. $\forall i \in \{1, \cdots, m_k\}$, one has

$$\tau_n(k) = \{\mathbf{T}^{k,l}, \mathbf{Z}^{k,l} = \{\mathbf{z}_j(k_0), \cdots, \mathbf{z}_i(k)\} \tag{24.28}$$

24.4.2 IMM with only one road segment constraint

The IMM is an algorithm for combining states hypotheses from multiple filter models to get a better state estimate when the target is maneuvering. IMM is near optimal with a reasonable complexity. In section 24.2.3, a constrained motion model i to segment s, noted $M_s^i(k)$, is defined. Here we extend the segment constraint to the different dynamic models (among a set of $r+1$ motion models) that a target can follow. The model indexed by $r = 0$ is the stop model. The transition between the models is a Markovian process. It is evident that when the target moves from one segment to the next, the set of dynamic models changes. In a conventionnal IMM estimator [1], the likelihood function of a model i is given, for a track $\mathbf{T}^{k,l}$, associated with the j-th measurement, $j \in \{0, 1, \ldots, m_k\}$ by:

$$\Lambda_i^l(k) = p\{\mathbf{z}_j(k) | M_s^i(k), \mathbf{Z}^{k-1,n}\}, \quad i = 0, 1, \ldots, r \tag{24.29}$$

where $\mathbf{Z}^{k-1,n}$ is the subsequence of measurements associated with the track $\mathbf{T}^{k,l}$.

Using the IMM estimator with a stop motion model, we get the likelihood function of the moving target mode for $i = 1, \ldots, r$ and for $j \in \{0, 1, \ldots, m_k\}$ by:

$$\Lambda_i^l(k) = P_D \cdot p\{\mathbf{z}_j(k) | M_s^i(k), \mathbf{Z}^{k-1,n}\} \cdot (1 - \delta_{m_j,0}) + (1 - P_D) \cdot \delta_{m_j,0} \tag{24.30}$$

while the likelihood of the stopped target mode (*i.e.* $r = 0$) is:

$$\Lambda_0^l(k) = p\{\mathbf{z}_j(k) | M_0^i(k), \mathbf{Z}^{k-1,n}\} = \delta_{m_j,0} \tag{24.31}$$

where $\delta_{m_j,0}$ is the Kronecker function defined by $\delta_{m_j,0} = 1$ if $m_j = 0$ and $\delta_{m_j,0} = 0$ whenever $m_j \neq 0$.

The combined/global likelihood function $\Lambda(k)$ of a track including a stop-model is then given by:

$$\Lambda^l(k) = \sum_{i=0}^{r} \Lambda_i^l(k) \cdot \mu_i(k|k-1) \tag{24.32}$$

where $\mu_i(k|k-1)$ is the predicted model probabilities [2].

The steps of the IMM under road segment s constraint are the same as for the classical IMM :

1. Step 1. Under the assumption of several possible models for segment s as defined previously, the mixing probabilities are given for i and j in $\{0, 1, \ldots, r\}$ by:

$$\mu_{i|j}(k-1|k-1) = \frac{p_{ij} \cdot \mu_i(k-1)}{\bar{c}_j} \tag{24.33}$$

where $\bar{c}_j$ is a normalizing factor. The probability of model switch depends on the Markov chain according to the transition probability p_{ij}. It is important to note that the transition probability does not depend on the constraint s.

2. Step 2. The mixing probabilities above are used to weight the initial state estimates in order to present to the model filters the mixed estimates. The mixed estimate of the target state under the road segment s constraint is defined for $i = 0, 1, \ldots, r$ by:

$$\hat{\mathbf{x}}^{0,l}_{i,s}(k-1|k-1) = \sum_{j=0}^{r} \hat{\mathbf{x}}^{l}_{j,s}(k-1|k-1) \cdot \mu_{i|j}(k-1|k-1) \tag{24.34}$$

The covariance corresponding to the estimation error is:

$$\begin{aligned}\mathbf{P}^{0,l}_{i,s}(k-1|k-1) = \sum_{j=0}^{r} \mu_{i|j}(k-1|k-1) \cdot [\mathbf{P}^{0,l}_{j,s}(k-1|k-1) + \\ (\hat{\mathbf{x}}_{j,s}(k-1|k-1) - \hat{\mathbf{x}}^{0,l}_{i,s}(k-1|k-1)) \cdot \\ (\hat{\mathbf{x}}_{j,s}(k-1|k-1) - \hat{\mathbf{x}}^{0,l}_{i,s}(k-1|k-1))']\end{aligned} \tag{24.35}$$

Despite of the constraint on local estimated states, the mixed estimated states do not belong to the road section s. Nevertheless, the state transition (24.5) matrix projects the mixed estimate on the road section.

3. Step 3. The motion models are constrained to the associated road segment. Each constrained mixed estimate (24.34) is predicted and associated to one new segment or several (in crossroad case) new ones, therefore the dynamics are modified according to the new segments. The mixed estimates (24.34) and (24.35) are used as inputs to the filter matched to M^i_s, which uses the MTI report associated to the track $\mathbf{T}^{k,l}$ to yield $\hat{\mathbf{x}}^{l}_{i,s}(k|k)$, $\mathbf{P}^{l}_{i,s}(k|k)$ and the corresponding likelihood (24.32).

4. Step 4. The model probability update is done for $i = 0, 1, \ldots, r$ as follows:

$$\mu_i(k) = \frac{1}{c} \cdot \Lambda^l_i(k) \cdot \bar{c}_i \tag{24.36}$$

where c is a normalization coefficient and $\bar{c}_i$ is given in (24.33).

5. Step 5. The combined state estimate, called global state estimate, is the sum of each constrained local state estimate weighted by the model probability, i.e.

$$\hat{\mathbf{x}}^{l}(k|k) = \sum_{i=0}^{r} \mu_i(k)\hat{\mathbf{x}}^{l}_{i,s}(k|k) \tag{24.37}$$

Here, one has presented briefly the principle of the IMM algorithm constrained to only one road segment s. However, a road section is composed with several road segments. When the target is making a transition from one segment to another, the problem is to choose the segments with the corresponding motion models that can better fit the target dynamics. The choice of a segment implies the construction of the directional process noise. That is why the IMM motions model set varies with the road network configuration and VS-IMM offers a better solution for ground target tracking on road networks as explained in next sections.

24.4.3 Variation of the set of constrained motion models

In the previous subsection, we have proposed an IMM with a given/fixed motion model set. We have noted that the predicted state could give a local estimate on another road segment than the segment associated to the motion model (a road turn for example). The change to another road segment causes the generation of a new constrained motion models. In literature, several approaches are proposed to deal with the constrained motion models [9, 15]. In [13], we have proposed an approach to activate the most probable road segments sets. Based on the work of Li [1], we consider $r+1$ oriented graphs which depend on the road network topology. For each graph i, $i = 0, 1, \ldots, r$, each node is a constrained motion model M^i_s. The nodes are connected to each other according to the road network configuration. For instance, if we consider a road section composed by three road segments s_1, s_2, s_3, the i^{th} associated graph is composed by three nodes ($M^i_{s_1}$, $M^i_{s_2}$ and $M^i_{s_3}$) where the nodes $M^i_{s_1}$ and $M^i_{s_3}$ are connected with the node $M^i_{s_2}$. In [13], the activation of the motion model at the current time depends on the local predicted states $\hat{\mathbf{x}}^{l}_{i,s}(k|k-1)$ location of the track $\mathbf{T}^{k,l}$. Consequently, we obtain a finite set of $r+1$ motion models constrained to a road section Ro_p (we recall that a road section is a set of connected road segments).

However, an ambiguity arises when there are several road sections (*i.e.* when the target approaches a crossroad). In fact, the number of constrained motion models grows up with the number of road sections present in the crossroad/junction. If we consider the $r+1$ graphs, the activation of the constrained motion model is done according to the predicted states location. Consequently the number of motion models increases with the number of road sections. We obtain several constrained motion model sets. Each set is composed of $r+1$ models constrained to road segments which belong to the road section. In order to select the most probable motion model set (*i.e.* in order to know on which road section the target is moving on), a sequential

probability ratio test named RSS-SPRT is proposed in [13] in order to select the road section taken by the target.

We consider that a hypothesis corresponds to one road section involved in the crossroad. At the current time k, if there are N_k road sections Ro_p at the intersection, we consider all N_k hypotheses. So for each hypothesis h, associated to a given road section, there is one IMM with an appropriate constrained motion models set. The IMM outputs are sequentially evaluated. However, one measurement iteration is not sufficient to choose the right hypothesis. The probability $\mu_h(k)$ of h is derived based on the likelihood function and the transition matrix between the road segments. The combined likelihood (24.32) of a constrained models set and for a hypothesis h, $h = 1, \ldots, N_k$ is denoted Λ_h. Mathematically, $\mu_h(k)$ is defined according to the road section probability [13] for $h = 1, \ldots, N_k$ by:

$$\mu_h(k) = \frac{1}{c} \cdot \Lambda_h(k) \cdot \sum_{\bar{h} \in \{1,\ldots,N_{k-1}\}} \Omega_{\bar{h},h}(k-1) \cdot \mu_{\bar{h}}(k-1) \tag{24.38}$$

The matrix component $\Omega_{\bar{h},h}$ represents the probability transition between the roads associated respectively to the hypotheses h and $\bar{h}$. In fact, if the road is a highway and the road section is also a highway, the transition probability is high. On the contrary, if the road is a highway and the road section is a byway the transistion probability is small. The probability $\mu_{\bar{h}}(k-1)$ is the probability of hypothesis $\bar{h}$ at the time $k-1$ (*i.e.* the probability of the previous road section where the target was moving on). Wald's sequential probability ratio test [20] (SPRT) for choosing the adequate road segment and activate the correct constrained motion model set at current time k is the following:

- Accept hypothesis h if for all $h' \neq h$, $h' \in \{1, \ldots, N_k\}$:

$$\frac{\mu_h(k)}{\mu_{h'}(k)} \geq B \tag{24.39}$$

- Reject hypothesis h if for all $h' \neq h$, $h' \in \{1, \ldots, N_k\}$:

$$\frac{\mu_h(k)}{\mu_{h'}(k)} \leq A \tag{24.40}$$

- Go to the next cycle and wait for one more measurement and continue the test until one hypothesis is accepted by the SPRT. The thresholds A and B are given in [5, 20]. For a faster test see the MSP-SPRT [1] based on probabilities classification.

24.4.4 VS-IMMC within the SB-MHT

We briefly describe the main steps of the VS-IMMC SB-MHT. More details can be found in chapter 16 of [5].

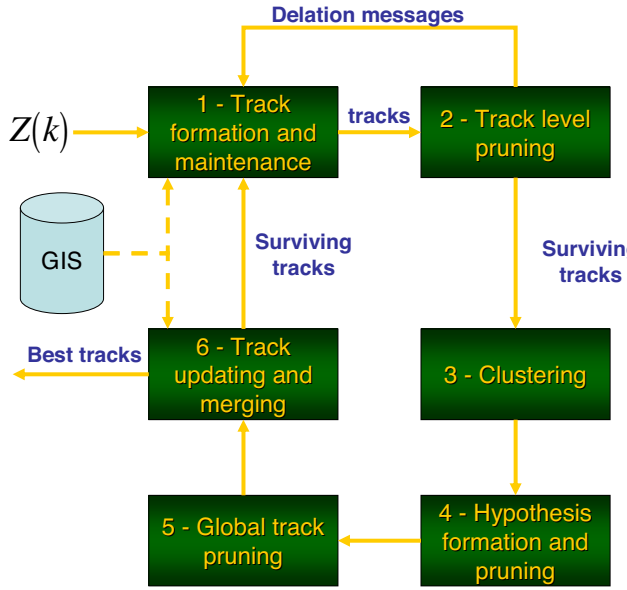

Figure 24.2: Track-oriented MHT logic flowchart with GIS.

1. The first functional block of the SB-MHT shown in figure 24.2 is the track confirmation and the track maintenance. When the new set $\mathbf{Z}(k)$ of measurements is received, a standard gating procedure [2] is applied in order to determine the viable MTI reports to track pairings. The existing tracks are updated with VS-IMMC and extrapolated confirmed tracks are formed. When the track is not updated with MTI reports, the stop motion model is activated.

2. In order to palliate the association problem, we need a probabilistic expression for the evaluation of the track formation hypotheses that includes all aspects of the data association problem. It is convenient to use the log-likelihood ratio (LLR) or track score of a track $\mathbf{T}^{k,l}$ which can be expressed at current time k in the following recursive form [5]:

$$L^l(k) = L^s(k-1) + \Delta L^l(k) \tag{24.41}$$

with

$$\Delta(k) = \ln(\frac{\Lambda^l(k)}{\lambda_{fa}}) \tag{24.42}$$

and

$$L(0) = \ln(\frac{\lambda_{fa}}{\lambda_{fa} + \lambda_{nt}}) \tag{24.43}$$

where λ_{fa} and λ_{nt} are respectively the false alarm rate and the new target rate per unit of surveillance volume. After the track score calculation of the track $\mathbf{T}^{k,l}$, the SPRT is used to set up the track status either as deleted, tentative or confirmed track. The tracks that fail the test are deleted and the surviving tracks are kept for the next stage.

3. The process of clustering is the collection of all tracks that are linked by a common measurement. The clustering technique is used to limit the number of hypotheses to generate and therefore to reduce the complexity. The result of clustering is a list of tracks that are interacting. The next step is to form hypotheses of compatible tracks.

4. For each cluster, in the fourth level, multiple coherent hypotheses are formed to represent the different compatible tracks scenarios. Each hypothesis is evaluated according to the track score function associated to the differents tracks. Then, a technique is required in order to find the hypotheses set that represents the most likely tracks collection. The unlikely hypotheses and associated tracks are deleted by a pruning process and only the N_{Hypo} best hypotheses are conserved.

5. For each track, the *a posteriori* probability is computed and a well known *N-Scan* pruning approach [5] is used to select and delete the confirmed tracks. With this approach the most likely track is selected to reduce the number of tracks. But the *N-Scan* technique combined with the constraint implies that other tracks hypotheses (*i.e.* constrained on other road segments) are arbitrary deleted. That is why, we must modify the *N-Scan* pruning approach in order to select the N_k best tracks on each N_k road sections.

6. Wald's SPRT proposed in section 24.4.3 is used to delete the unlikely hypotheses among the N_k hypotheses. The tracks are then updated and projected on the road network. In order to reduce the number of track to keep in the memory of the computer, a merging technique (selection of the most probable tracks which have common measurements) is also implemented.

24.4.5 OOSM algorithm

The data fusion that operates in a centralized architecture suffers of delayed measurement due to communication data links, time algorithms execution, data quantity,... In order to avoid reordering and reprocessing an entire sequence of measurements for real-time application, the delayed measurements are processed as out-of-sequence

measurements (OOSM). The algorithm used in this work is described in [3]. In addition, according to the road network constraint, the state retrodiction step is done on the road.

24.5 Target type tracking

In [6], Blasch and Kahler fused identification attribute given by EO/IR sensors with position measurement. The fusion was used in the validation gate process to select only the measurement according to the usual kinematic criterion and the belief on the identification attribute. Our approach is different since one uses the belief on the identification attribute to revise the LLR (24.42) with the *posterior* pignistic probability on the target type. We recall briefly the Target Type Tracking (TTT) principle and explain how to improve VS-IMMC SB-MHT with target ID information. TTT is based on the sequential combination (fusion) of the predicted belief of the type of the track with the current "belief measurement" obtained from the target classifier decision. Results depends on the quality of the classifier characterized by its confusion matrix (assumed to be known at least partially as specified by STANAG). The adopted combination rule is the so-called Proportional Conflict Redistribution rule no 5 (PCR5) developed in the DSmT (Dezert Smarandache Theory) framework since it deals efficiently with (potentially high) conflicting information. A detailed presentation with examples can be found in [7, 16]. This choice is motivated in this typical application because in dense traffic scenarios, the VS-IMMC SB-MHT only based on kinematic information can be deficient during maneuvers and crossroads. Let's recall first what the PCR5 fusion rule is and then briefly the principle of the (single-sensor based) Target Type Tracker.

24.5.1 PCR5 combination rule

Let $C_{Tot} = \{\theta_1, \ldots, \theta_n\}$ be a discrete finite set of n exhaustive elements and two distinct bodies of evidence providing basic belief assignments (bba's) $m_1(.)$ and $m_2(.)$ defined on the power set[3] of C_{Tot}. The idea behind the Proportional Conflict Redistribution (PCR) rules [16] is to transfer (total or partial) conflicting masses of belief to non-empty sets involved in the conflicts proportionally with respect to the masses assigned to them by sources. The way the conflicting mass is redistributed yields actually several versions of PCR rules, but PCR5 (i.e. PCR rule # 5) does the most exact redistribution of conflicting mass to non-empty sets following the logic of the conjunctive rule and is well adapted for a sequential fusion. It does a better redistribution of the conflicting mass than other rules since it goes backwards on the tracks of the conjunctive rule and redistributes the conflicting mass only to the sets involved in the conflict and proportionally to their masses put in the conflict. The PCR5 formula for $s \geq 2$ sources is given in [16]. For the combination of only two

[3]In our MTT applications, we will assume Shafer's model for the frame C_{Tot} of target ID which means that elements of Θ are assumed truly exclusive.

sources (useful for sequential fusion in our application) when working with Shafer's model, it is given by $m_{PCR5}(\emptyset) = 0$ and $\forall X \in 2^{C_{Tot}} \setminus \{\emptyset\}$

$$m_{PCR5}(X) = m_{12}(X) + \sum_{\substack{Y \in 2^{C_{Tot}} \setminus \{X\} \\ X \cap Y = \emptyset}} \left[\frac{m_1(X)^2 m_2(Y)}{m_1(X) + m_2(Y)} + \frac{m_2(X)^2 m_1(Y)}{m_2(X) + m_1(Y)}\right] \quad (24.44)$$

where $m_{12}(X)$ corresponds to the conjunctive consensus on X between the two sources (i.e. our a prior bba on target ID available at time $k-1$ and our current *observed* bba on target ID at time k) and where all denominators are different from zero. If a denominator is zero, that fraction is discarded.

24.5.2 Principle of the target type tracker

To estimate the true target type, denoted $type(k)$, at time k from the sequence of declarations $c(1)$, $c(2)$, $\ldots c(k)$ done by the unreliable classifier[4] up to time k. To build an estimator $\widehat{type}(k)$ of $type(k)$, we use the general principle of the Target Type Tracker (TTT) developed in [7] which consists in the following steps:

- a) Initialization step (*i.e.* $k = 0$). Select the target type frame $C_{Tot} = \{\theta_1, \ldots, \theta_n\}$ and set the prior bba $m^-(.)$ as vacuous belief assignment, i.e $m^-(\theta_1 \cup \ldots \cup \theta_n) = 1$ since one has no information about the first observed target type.

- b) Generation of the current bba $m_{obs}(.)$ from the current classifier declaration $c(k)$ based on attribute measurement. At this step, one takes $m_{obs}(c(k)) = P\{c(k)\} = C_{c(k)c(k)}$ and all the unassigned mass $1 - m_{obs}(c(k))$ is then committed to total ignorance $\theta_1 \cup \ldots \cup \theta_n$. $C_{c(k)c(k)}$ is the element of the known confusion matrix $\mathbf{C}$ of the classifier indexed by $c(k)c(k)$.

- c) Combination of current bba $m_{obs}(.)$ with prior bba $m^-(.)$ to get the estimation of the current bba $m(.)$. Symbolically we write the generic fusion operator as $\oplus$, so that $m(.) = [m_{obs} \oplus m^-](.) = [m^- \oplus m_{obs}](.)$. The combination $\oplus$ is done according to the PCR5 rule, *i.e.* $m(.) = m_{PCR5}(.)$.

- d) Estimation of True Target Type is obtained from $m(.)$ by taking the singleton of C_{Tot}, *i.e.* a Target Type, having the maximum of belief (or eventually the maximum Pignistic Probability[5]).

$$\widehat{type}(k) = \underset{A \in C_{Tot}}{argmax}(BetP\{A\}) \quad (24.45)$$

[4]Here we consider only one source of information/classifier, say based either on the EO/IR sensor, or on a video sensor by example. The multi-source case is discussed in section 24.5.3.

[5]The maximum of the pignistic probability has been used in this preliminary work, but the maximum of $DSmP(.)$ presented in the Chapter [**?**] in this volume will be tested in further developments.

The Pignistic Probability is used to estimate the probability to obtain the type $\theta_i \in C_{Tot}$ given the previous target type estimate $\widehat{type}(k-1)$.

$$BetP\{\theta_i\} = P\{\widehat{type}(k) = \theta_i | \widehat{type}(k-1)\} \tag{24.46}$$

- e) set $m^-(.) = m(.)$; do $k = k+1$ and go back to step b).

Naturally, in order to revise the LLR (24.42) in our MTT systems for taking into account the estimation of belief of target ID coming from the Target Type Trackers, we transform the resulting bba $m(.) = [m^- \oplus m_{obs}](.)$ available at each time k into a probability measure. In this work, we use the classical pignistic transformation defined by [17]:

$$BetP\{A\} = \sum_{X \in 2^\Theta} \frac{|X \cap A|}{|X|} m(X) \tag{24.47}$$

24.5.3 Working with multiple sensors

Since in our application, we work with different sensors (*i.e.* MTI and Video EO/IR sensors), one has to deal with the frames of discernment C_{MTI} and C_{video} defined in section 24.4. Therefore we need to adapt the (single-sensor based) TTT to the multi-sensor case. We first adapt the frame C_{MTI} to C_{video} and then, we extend the principle of TTT to combine multiple bba's (typically here $m_{obs}^{MTI}(.)$ and $m_{obs}^{Video}(.)$) with prior target ID bba $m^-(.)$ to get finally the updated global bba $m(.)$ at each time k. The proposed approach can be theoretically extended to any number of sensors. When no information is available from a given sensor, we take as related bba the vacuous mass of belief which represents the total ignorant source because this doesn't change the result of the fusion rule [16] (which is a good property to satisfy). For mapping C_{MTI} to C_{video}, we use a (human refinement) process such that each element of C_{MTI} can be associated at least to one element of C_{video}. In this work, the delay on the type information provided by the video sensor is not taking into account to update the global bba $m(.)$. All type information (delayed or not provided by MTI and video sensors) are considered as bba $m_{obs}(.)$ available for the current update. The explicit introduction of delay of the out of sequence video information is under investigations.

24.5.4 Data attributes in the VS IMMC

To improve the target tracking process, the introduction of the target type probability is done in the likelihood calculation. For this, we consider the measurement $\mathbf{z}_j^\star(k)(\forall j \in \{1, \ldots, m_k\})$ described in (24.22) and (24.26). With the assumption that the kinematic and classification observations are independant, it is easy to proove that the new combined likelihood Λ_N^l associated with a track $\mathbf{T}^{k,l}$ is the product of the kinematic likelihood (24.32) with the classification probability in the manner that:

$$\Lambda_N^l(k) = \Lambda^l(k) \cdot P\{\widehat{type}(k) | \widehat{type}(k-1)\} \tag{24.48}$$

where the probability $P\{\widehat{type}(k)|\widehat{type}(k-1)\}$ is chosen as the pignistic probability value on the declared target type $\widehat{type}(k)$ derived from the updated mass of belief $m(.)$ according to our target type tracker.

24.6 Simulations and results

24.6.1 Scenario description

To evaluate the performances of the VS-IMMC SB-MHT with the attribute type information, we consider 10 maneuvering (acceleration, deceleration, stop) targets on a real road network (see figure 24.3). The 10 target types are given by (24.25).

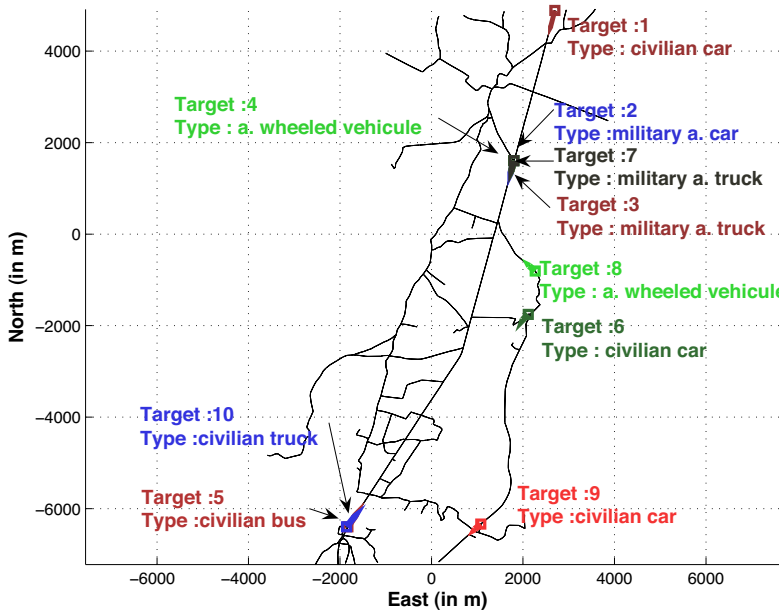

Figure 24.3: Targets trajectories.

The target 1 is passing the military vehicles 2, 3, 4 and 7. Targets 2, 3, 4 and 7 start from the same starting point.The target 2 is passing the vehicles 3 and 7 in the manner that it places in front of the convoy. The targets 5, 6, 9 and 10 are civilian vehicles and are crossing the targets 1, 2, 3 and 7 at several junctions. The goal of this simulation is to reduce the association complexity by taking into account the road network topology and the attribute types given by heterogeneous sensors. In this scenario, we consider one GMTI sensor located at $(-50km, -60km)$ at $4000m$ in elevation (figure 24.4) and one UAV located at $(-100m, -100m)$ (figure 24.5) at $1200m$ in elevation and 5 UGS distributed on the ground (figure 24.6).

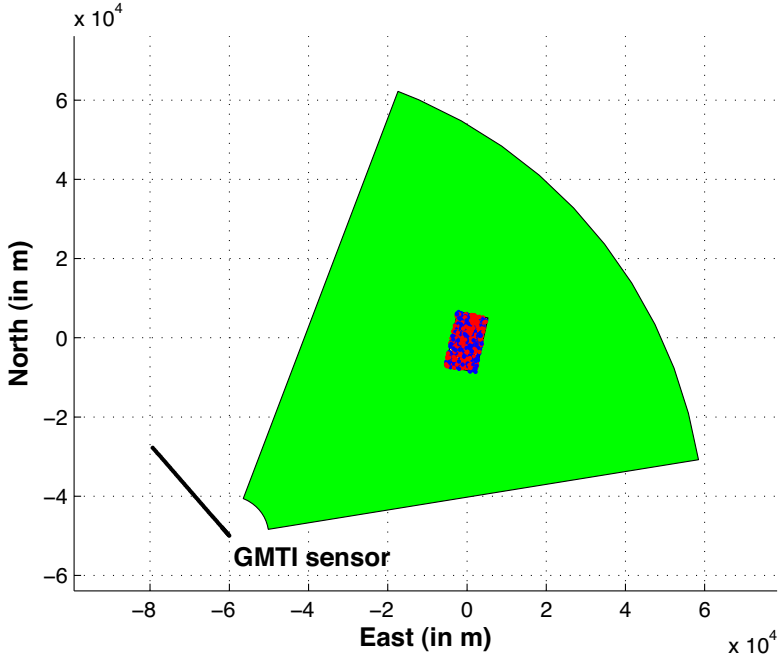

Figure 24.4: GMTI sensor trajectory and cumulated MTI reports.

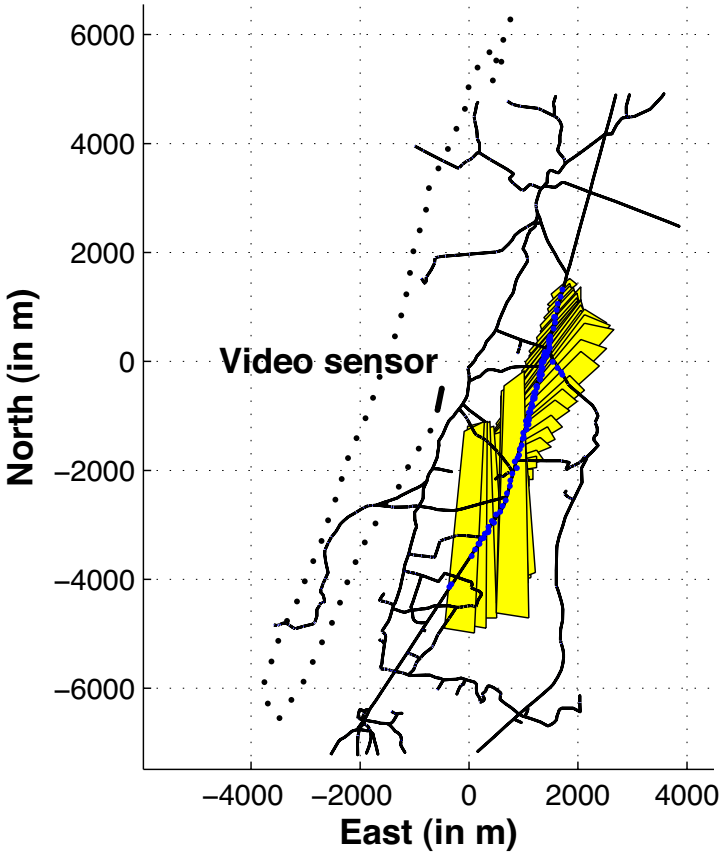

Figure 24.5: UAV trajectory with video sensor ground coverage.

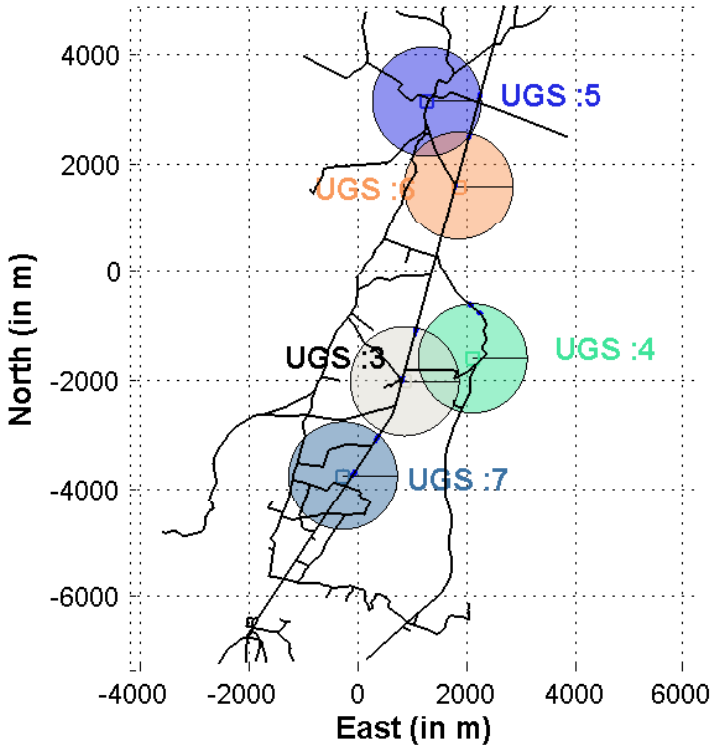

Figure 24.6: UGS positions with field of view.

The GMTI sensor tracks the 10 targets at every 10 seconds with $20\,m$, $0.0008\,rad$ and $1m \cdot s^{-1}$ range, cross-range and range-rate measurements standard deviation respectively. The detection probability P_D is equal to 0.9 and the MDV (Minimal Detectable Velocity) fixed at $1\,m/s$. The false alarms density is fixed ($\lambda_{fa} = 10^{-8}$). The confusion matrix described in part 24.5.2 is given by:

$$\mathbf{C}_{MTI} = \text{diag}([0.8\ 0.7\ 0.9]) \tag{24.49}$$

This confusion matrix is only used to simulate the target type probability of the GMTI sensor. The data obtained by UAV are given at 10 seconds with $10\,m$ standard deviation in X an Y direction from the TCF. The time delay of the video data is constant and equal to 11 seconds. The detection probability P_D is equal to 0.9. The human operator only selects for each video report a type defined by (24.25). In our simulations, the target type probability depends on the sensor resolution. For this, we consider the volume V_{video} of the sensor area surveillance on the ground. The diagonal terms of the confusion matrix $\mathbf{C}_{video}$ are equal to $P\{c(k)\}$ where $P\{c(k)\}$ is defined by:

$$P\{c(k)\} = \begin{cases} 0.90\ if\ V_{video} \leq 10^6 m^2 \\ 0.75\ if\ 10^6 m^2 < V_{video} \leq 10^8 m^2 \\ 0.50\ if\ V_{video} > 10^8 m^2 \end{cases} \tag{24.50}$$

For the UGS, the target detection is done if only the target is located under the minimal range detection (MRD). The MRD is fixed for the 5 UGS at 1000 m and each sensor gives delayed measurement every seconds. The time delay is also equal to 11 seconds. The UGS specificity is to give only one target detection during 4 seconds in order to detect another target. We recall that there is no false alarm for this sensor. Based on [6], the target type probability depends on α (*i.e.* the target orientation towards the UGS). The more the target orientation is orthogonal to the sensor line of sight, the more the target type probability increases. The diagonal terms of the confusion matrix $\mathbf{C}_{UGS}$ are equal to $P\{c(k)\}$ where $P\{c(k)\}$ is defined by:

$$P\{c(k)\} = \begin{cases} 0.90 & if\ \frac{5\pi}{6} \leq \alpha \leq \frac{\pi}{6} \\ 0.50 & otherwise \end{cases} \tag{24.51}$$

For each detected target, a uniform random number $u \sim U([0,1])$ is drawn. If u is greater than the true target type probability of the confusion matrix, a wrong target type is declared for the ID report and used with its associated target type probability. The targets are scanned at different times by the sensors (figure 24.7).

24.6.2 Filter parameters

We consider three motion models M^i, $i = 0, 1, 2$ which are respectively a stop model M_0 when the target is assumed to have a zero velocity, a constant velocity model M^1 with a low uncertainty, and a constant velocity model M^2 with a high uncertainty (modeled by a strong noise). The parameters of the IMM are the following: for the

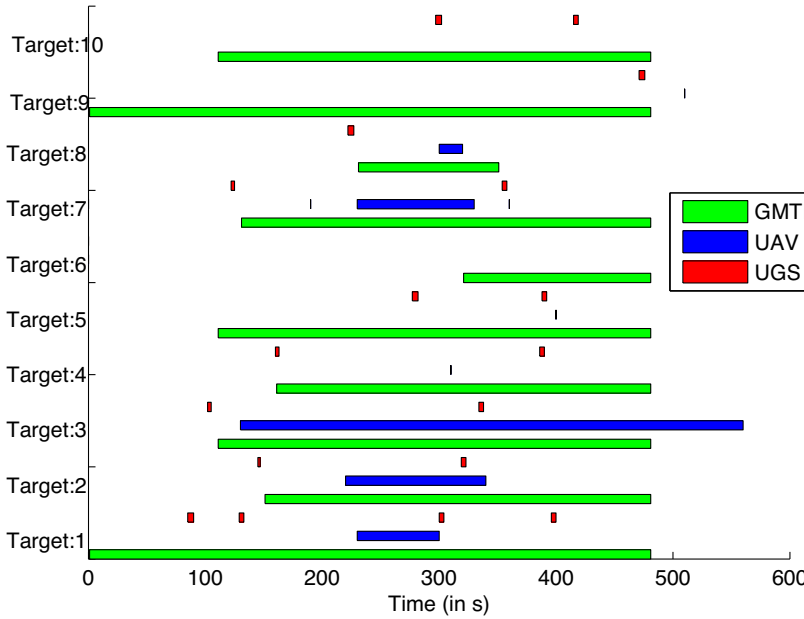

Figure 24.7: Target's sensor illumination.

motion model M^1, standard deviations (along and orthogonal to the road segment) are equals to 0.05 $m \cdot s^{-2}$), the constrained constant velocity model M^2 has a high standard deviation to adapt the dynamics to the target maneuver (the standard deviation along and orthogonal to the road segment are respectively equal to 0.8 $m \cdot s^{-2}$ and 0.4 $m \cdot s^{-2}$) and the stop motion model M^0 has a standard deviation equals to zero. These constrained motion models are however adapted to follow the road network topology. The transition matrix and the SB-MHT parameters are those taken in [14].

24.6.3 Results

For each confirmed track given by the VS-IMMC SB-MHT, a test is used to associate a track to the most probable target. The target tracking goal is to track as long as possible the target with one track. To evaluate the track maintenance, we use the track length ratio criterion, the averaged root mean square error (noted ARMSE) for each target and the track purity and the type purity (only for the tracks ob-

tained with PCR5) [14]. We obtain for each target the averaged track length ratio ($\forall n \in \{1, ..., 10\}\}$):

$$R_n = \sum_{k=1}^{N_{mc}} \frac{l_n}{N_{mc} \cdot L_n} \tag{24.52}$$

where N_{mc} is the number of Monte-Carlo runs, l_n is the mean track length associated the target n and L_n is the length of the true target trajectory.

In addition to the track length ratio criterion, we calculte the ARMSE for each target, the track purity and the type purity (only for the tracks obtained with PCR5). The ARMSE is the root mean square error averaged on the time. The track purity is the ratio between the sum of correct association number on the track length and the type purity is the ratio between the sum of true type decision number on the track length. These measures of performances are averaged on the number Monte-Carlo runs. In this simulation we have used $N_{mc} = 50$ Monte-Carlo runs.

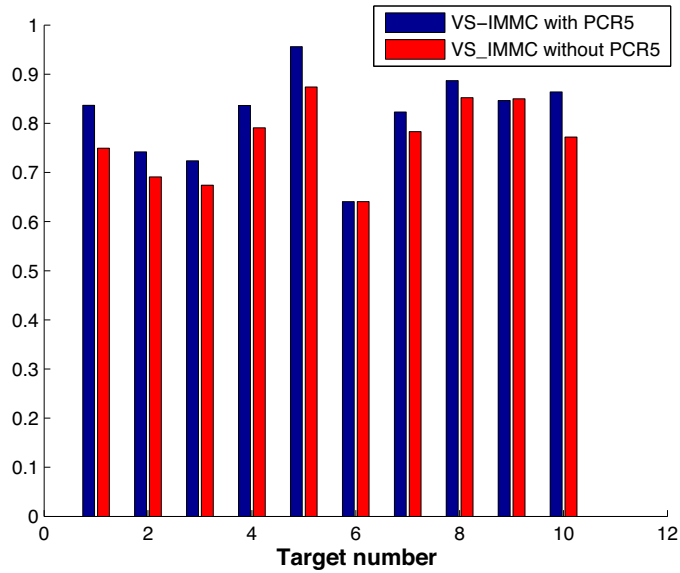

Figure 24.8: Track length ratio.

On the figure 24.8, one sees that the track length ratio becomes better with the PCR5 than without as expected for the target 6. When the targets 1 and 2 are passing the targets 3, 4 and 7, an association ambiguity arises to associate the tracks

with the correct measurements. This is due to the close formation between targets with the GMTI sensor resolution and the road network configureation with junctions. Sometimes tracks are lost with the VS IMMC SB-MHT without the PCR5. Then new tracks for each targets are built. That is why, the track purity of the VS IMMC SB-MHT without PCR5 (see Table 24.1) is smaller than the track purity with PCR5 (see Table 24.2). So, the track precision, given by the ARMSE criterion, is better with the PCR5. For the target 6 results, this target is only scanned by the GMTI sensor and its associated performances are equivalent for both algorithms. Then, if there is no IMINT information and no interaction between targets, the performances of the algorithm with PCR5 are the same as without PCR5.

Despite of the PCR5 improvement on the target tracking, the difference of performances between the algorithms is not significant. If there is an interaction between IMINT and GMTI information, we can see a gain on the track length ratio or track purity of 10% with PCR5. This small difference is due to the good constrained state estimation. The estimated target states have a good precision because the target tracking is done by taking into account the road segments location and the good performances of the OOSM approach. So, it implies a substantial improvement of the target-to-track association. In addition, on Table 24.2, the type purity based on PCR5 is derived from the maximum of $BetP$ criterion. But $BetP$ is computed according the set C_{video} (24.25) and if the track receives only MTI reports the choice on the target type is arbitrary for the tracked vehicles of C_{MTI} (24.21). In fact, a tracked vehicle can be 6 elements of (24.25). So the probability $BetP$ on the 6 tracked vehicles of (24.25) is the same. The selection of the maximum of $BetP$ has no meaning because in such case the maximum becomes arbitrary. This explains the bad track purity of targets 6 and 9.

Target	ARMSE	Track purity	Type purity
1	14.82	0.70	none
2	16.62	0.62	none
3	15.61	0.61	none
4	22.54	0.77	none
5	16.25	0.85	none
6	18.68	0.64	none
7	14.45	0.72	none
8	17.51	0.84	none
9	19.23	0.85	none
10	17.40	0.75	none

Table 24.1: Tracking results (VSIMMC without PCR5).

Target	ARMSE	Track purity	Type purity
1	14.37	0.78	0.64
2	15.77	0.66	0.62
3	15.60	0.61	0.59
4	21.10	0.81	0.81
5	15.88	0.94	0.55
6	18.68	0.64	0.02
7	14.22	0.76	0.76
8	17.38	0.87	0.87
9	19.20	0.85	0.05
10	17.17	0.83	0.46

Table 24.2: Tracking results (VSIMMC and PCR5).

24.7 Conclusion

In this chapter, we have presented a new approach to improve VS IMMC SB-MHT by introducing the data fusion with several heterogeneous sensors. Starting from a centralized architecture, the MTI and IMINT reports are fused by taking into account the road network information and the OOSM algorithm for delayed measurements. The VS IMMC SB-MHT is enlarged by introducing in the data association process the type information defined in the STANAG 4607 and an IMINT attribute set. The estimation of the Target ID probability is done from the updated/current attribute mass of belief using the Proportional Conflict Redistribution rule no. 5 developed in DSmT framework and according to the Target Type Tracker (TTT) recently developed by the authors. The Target ID probability once obtained is then introduced in the track score computation in order to improve the likelihoods of each data association hypothesis of the SB-MHT. Our preliminary results show an improvement of the performances of the VS-IMMC SB-MHT when the type information is processed by our PCR5-based Target Type Tracker. In this work, we did not distinguish undelayed from delayed sensor reports in the TTT update. This problem is under investigations and offers new perspectives to find a solution for dealing efficiently with the time delay of the identification data attributes and to improve the performances. One simple solution would be to use a forgetting factor of the delayed type information but other solutions seem also possible to explore and need to be evaluated. Some works need also to be done to use the operational ontologic APP-6A for the heterogeneous type information. Actually, the frame of the IMINT type information is bigger than the one used in this chapter and the IMINT type information can be given at different granularity levels. As a third perspective, we envisage to use both the type and contextual information in order to recognize the tracks losts in the terrain masks which represent the possible target occultations due to the terrain topography in real environments.

24.8 References

[1] Y. Bar-Shalom, D. Blair, *Multitarget multisensor tracking: Applications and Advances*, Vol. III, Artech House, 2000.

[2] Y. Bar-Shalom, X. R. Li and T. Kirubarajan, *Estimation with applications to tracking and navigation: algorithms and softaware for information extraction*, Wiley, New York, 2001.

[3] Y. Bar-Shalom, H. Chen, *IMM estimator with out-of-sequence measurements'*, IEEE Trans. on AES, Vol. 41, No. 1, pp. 90–98, January 2005.

[4] D.F. Bizup, D.E. Brown, *The over-extended Kalman filter - Don't use it!*, Proc. of ICIF, Fusion 2003, Cairns, Australia, July 2003.

[5] S.S. Blackman, R. Popoli, *Design and analysis of modern tracking systems*, Artech House, 1999.

[6] E. Blasch, B. Kahler, *Multiresolution EO/IR target tracking and identification*, Proc. of ICIF, Fusion 2005, Philadelphia, PA, USA, pp. 275–282, July 2005.

[7] J. Dezert, A. Tchamova, F. Smarandache and P.Konstantinova, *Target Type Tracking with PCR5 and Dempster's rules: A Comparative Analysis*, Proc. of ICIF, Fusion 2006, Firenze, Italy, July 2006.

[8] J. G. Herrero, J. A. B. Portas and J. R. C. Corredara, *Use of Map Information for target tracking on airport surface*, IEEE Trans., on AES, Vol. 39, no. 2, pp. 675–693, April 2003.

[9] T. Kirubarajan, Y. Bar-Shalom, K.R. Pattipati and I. Kadar, *Ground target tracking with topography-based variable structure IMM estimator*, Proc. of SPIE, signal and data processing of small targets, Vol. 3373, pp. 222–233, Jul. 1998.

[10] T. Kirubarajan, Y. Bar-Shalom, *Tracking evasive move-stop-move targets with an MTI radar using a VS-IMM estimator*, IEEE Trans. on AES, Vol. 39, No. 3, pp. 1098–1103, July 2003.

[11] NATO, *STANAG 4607 JAS (Edition 2) - NATO ground moving target indicator GMTI) format*, NSA0749(2007)-JAS/4607, August 2007.

[12] B. Pannetier, K. Benameur, V. Nimier and M. Rombaut, *Ground target tracking with road constraint*, Proc. of SPIE, sensor fusion and target recognition XIII, Volume 5429, April 2004.

[13] B. Pannetier, V. Nimier and M. Rombaut, *Multiple ground target tracking with a GMTI sensor*, Proc. of MFI 2006, pp .230–236, September 2006.

[14] B. Pannetier, J. Dezert and E. Pollard, *Improvement of multiple ground targets tracking with GMTI sensors and fusion identification attributes*, IEEE Aerospace Conference, pp. 1–13, March 2008.

[15] P.J. Shea, T. Zadra, D. Klamer, E. Frangione and R. Brouillard, *Improved state estimation trough use of roads in ground tracking*, Proc.of SPIE, Signal and Data Processing of Small Targets, Vol. 4048, pp. 321–332, July 2000.

[16] F. Smarandache, J. Dezert, (Editors), *Advances and Applications of DSmT for Information Fusion (Collected Works)*, Vol. 2, American Research Press, Rehobooth, U.S.A, 2006.

[17] Ph. Smets, *Data Fusion in the Transferable Belief Model*, Proc. of ICIF, Fusion 2000, pp. PS21–PS33, Paris, France, July 10-13, 2000.

[18] D.U. Thibault, *Commented APP-6A - Military symbols for land based systems*, Technical Note, DRDC Val Cartier, TN 2005-222, September 2005.

[19] M. Ulmke, W. Koch, *Road-map assisted ground moving target tracking*, IEEE Trans. on AES, Vol. 42, No. 4, pp. 1264–1274, October 2006.

[20] A. Wald, J. Wolfowitz, *Optimum character of the sequential probability ratio test*, Ann. Math. Stat., Vol. 19, pp. 326–339, 1948.

[21] J. G. Wang, T. Long and P.K. He, *A New Method of Incorporating Radial Velocity Measurement into Kalman Filter*, Proc. of SPIE, no. 18, pp. 414–416, 2002.